Video rate depth resolved two dimensionnal imaging through turbid media by femtosecond parametric amplification

Claude Doule, Thierry Lépine, Patrick Georges, Alain Brun

Video rate depth-resolved two-dimensional imaging through turbid media by femtosecond parametric amplification

C. Doulé, T. Lépine, P. Georges, and A. Brun

Laboratoire Charles Fabry de l'Institut d'Optique, Centre National de la Recherche Scientifique, Unité de Recherche Associée No. 8501, B.P. 147, 91403 Orsay Cedex, France

We report two-dimensional imaging through a liquid scattering medium by noncollinear femtosecond parametric amplification in a reflection configuration. The experiment presented permits direct observation at video rate of two-dimensional images with 24-μm depth resolution and 90-μm transverse resolution for an area with a 2.5-mm diameter on the object. These resolutions are achievable through a turbid phantom with a depth near 12 scattering mean free paths in double pass.   © 2000 Optical Society of America

OCIS codes: 170.6920, 170.7050, 190.7110.

In recent years, coherence domain imaging has been studied as a means of depth-resolved imaging in turbid media.[1-4] Optical coherence tomography can achieve *in vivo* imaging of biological tissues at video rate in a series of axial depth scans.[2] Other coherence-gated methods such as photorefractive holography[3] and full-field coherence tomography[4] directly produce two-dimensional (2-D) images for a given depth at video rate. With the development of femtosecond lasers, the use of time-gated imaging as a means of depth-resolved imaging should be investigated. These techniques are usually used in a transillumination configuration,[5-8] and little research has been done on depth-resolved imaging. For instance, using upconversion, Yan and Diels[9] achieved depth-resolved 2-D imaging through a turbid phantom with 80-fs pulses at 600 nm but with a lateral spatial resolution limited to 300 μm.

Previously,[7] point-to-point imaging was accomplished through a scattering medium with degenerate type I parametric amplification in the femtosecond regime. A grid with 500-μm bar spacing was transilluminated through a scattering medium of 20 mean free paths. However, the acquisition speed of the image was limited by the 10-Hz repetition rate of the laser. Even if the repetition rate had been increased to 1 kHz for the amplified laser chain, the number of points scanned on the object in 40 ms (European video rate) would have been limited to 40. To overcome this limitation we moved to a direct 2-D imaging configuration based on degenerate type II parametric amplification operating at video rate. The feasibility of high-resolution 2-D imaging by type II parametric amplification was previously shown in the picosecond regime in the transillumination configuration.[8] Furthermore, using femtosecond pulses, we were able to obtain a narrower time gating and to work in retroreflection with a high resolution of depth. In this Letter we present an experiment in which we use parametric amplification in a reflection configuration with femtosecond pulses at 800 nm (therapeutic window) to achieve high-resolution 2-D imaging at video rate.

In our experiment, short pulses are launched into a scattering medium. Time gating allows us to select retroreflections that correspond to a given depth. For this we use a Ti:sapphire laser system that delivers 300-μJ, 100-fs pulses near 800 nm at a 1-kHz repetition rate (Fig. 1). The pulses are frequency doubled in an 800-μm-long β-barium borate (BBO) crystal (type I) with an efficiency near 35%. The remaining *p*-polarized 800-nm beam is split off from the *s*-polarized blue pump beam (400 nm) and illuminates the object over an area 4 mm in diameter. The combination of a quarter-wave plate and a polarizing beam splitter isolates the reflected beam from the incoming beam. The object is imaged onto another 800-μm-long BBO crystal (type II) with an afocal system of 0.5× magnification. The width of the pump beam is reduced by a factor of 2 by an afocal system. The type II interaction of the pump beam and the signal beam in the second crystal creates an idler beam at 800 nm with polarization (*p* polarization) orthogonal to the signal polarization (*s* polarization). This idler beam is created only when the delay between the pump and the signal pulses is adjusted. During this time gate, the image formed in the type II BBO crystal by the signal beam is duplicated on the idler beam. Consequently, we can observe different slices in a scattering medium by moving the mirrors of the delay line. The pump beam and the signal beam, respectively, are
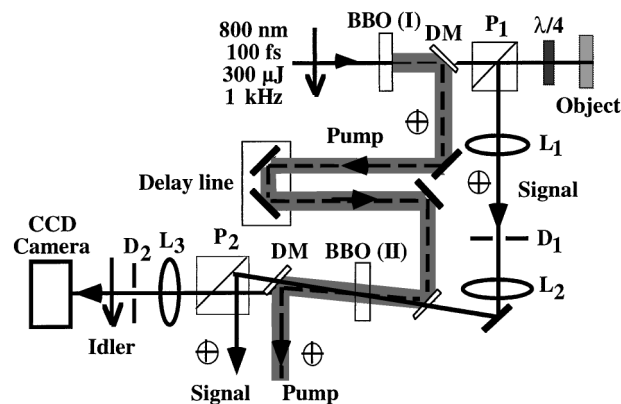

Fig. 1. Experimental setup: L$_i$, lenses; P$_i$, polarizing beam splitters; DM, dichroic mirror; D$_i$, diaphragms; ↑, polarization; ⊕, polarization.

© 2000 Optical Society of America

removed with a dichroic mirror and a polarizing beam splitter. Thus the image of the object formed with the idler beam on a CCD camera (8-bit Pulnix TM-765) is above a dark field. We chose the value of 800 μm for the type II BBO crystal length close to the theoretical interaction length of the three waves limited by the group-velocity mismatch. In consequence, the gain of the parametric process is only ~20%. Because of the rejection of the crossed polarizers (~40 dB), the time gating becomes efficient enough that we can extract the useful information carried by the idler beam from the total signal coming from the object.

To yield the most-resolved 2-D images, the parametric process must amplify the most spatial frequencies of the image. The phase-matching configuration must be noncritical in angle for both signal and idler beams. It was shown by Lantz et al.[10] that this noncritical phase-matching configuration occurs when the Poynting vectors of the signal and the idler beams are collinear. For a λ-degenerate type II interaction in a BBO crystal with a pump wavelength of 400 nm, this configuration corresponds to a 2° noncollinear interaction between the idler and the pump wave vectors. The angle (θ_p) between the optical axis of the BBO crystal and the pump beam is then near 41.5°. We adjusted the noncollinear interaction experimentally to improve the lateral spatial resolution. For this purpose we observed in the Fourier plane of lens L_3 the spatial frequency spectra of images of a reflecting diffuser (the object in Fig. 1) for different values of angle θ_p between the pump beam and the optical axis of the crystal. As shown in Fig. 2(a), for the collinear interaction ($\theta_p \approx 42.3°$) few spatial frequencies (≈ 0.008 μm^{-1}, corresponding to 130-μm lateral spatial resolution) are amplified in the critical direction parallel to the optical axis. The pump beam is at point A. By changing θ_p to 41.5° by a simple rotation of the crystal, we could enhance the width of the amplified spatial frequency spectrum in this critical direction [Fig. 2(b)]. Point B in Fig. 2(b) corresponds to the direction of the idler wave vector propagating in the crystal at an angle of 2° with respect to the pump wave vector. In this direction the phase-matching conditions are noncritical and the total amplified spatial frequency spectrum is a circle of radius $r_d = 0.025$ μm^{-1} [Fig. 2(b)], given a lateral spatial resolution of 40 μm. But, as shown in Fig. 2(b), part of the spectrum is cut off by the optics of our system. We could have corrected this problem by enhancing the angular acceptance of our optical system. However, we preferred to place the zero order of the image between points A and B and to amplify just half of the spectrum. In this way a spatial frequency spectrum equivalent to a half-circle of ≈ 0.021-μm^{-1} radius could be amplified, given an expected transverse resolution near 48 μm. This choice permits us to work closer to the collinear interaction with easier adjustments. Because of the imperfect rejection of the crossed polarizers (only 40 dB), we added spatial filtering with two diaphragms, D_1 and D_2, respectively, in the Fourier planes of lenses L_1 and L_3 (Fig. 1). D_1 and D_2 are, respectively, centered on the zero order of the images that correspond to the sig-

nal and the idler beams. Their diameters are the smallest compatible with the best transverse resolution. All the remaining portion of the signal beam that is not removed by the polarizer is stopped by diaphragm D_2 because of the noncollinear interaction. This spatial filtering removes all the detectable signal beam. The choice of noncollinear interaction enhances both the lateral spatial resolution and the rejection of the signal (>60 dB).

To measure the transverse resolution, we replaced the reflecting diffuser with a U.S. Air Force test target, without any scattering medium. In direct imaging with the s-polarized signal beam (polarizer P_1 in Fig. 1, rotated), element 4.3 (20.16 lines/mm) was the smallest detail (50 μm) that could be resolved. With the maximum amplified spatial frequency spectral width measured in the previous experiment taken into account, this element should have been resolved with the time-gated imaging. However, when we adjusted the noncollinear interaction to obtain the best possible images, the smallest resolved element was element 3.6 (14.3 lines/mm, corresponding to 70 μm). Aberrations that were due to inhomogeneities in the spatial profile of the pump could prevent the observation of the smallest details. The field observed on the object is ~2.5 mm in diameter (FWHM). According to the resolution, the number of resolved points on the object is thus near 1000. To evaluate the depth resolution, we measured the power of the idler beam for different positions of the delay line for a fixed position of the test target. We obtained a value of ~32 μm (FWHM) in air, which would be 24 μm in a medium with a group index of 1.33. This value is in good agreement with the theoretical evaluation of the duration of both the pump and the signal pulses in the second BBO crystal.

To validate the method for looking through a scattering medium, we performed an imaging of the U.S. Air Force target placed behind a 5-mm-thick cell filled with a suspension of 213-nm-diameter latex spheres in water ($N \approx 8.68 \times 10^{11}$ cm^{-3} and $g \approx 0.22$). Element 3.6 (70 μm) is still well resolved (Fig. 3). With the data given by the manufacturer, the calculation of the equivalent number of scattering mean free paths (mfp), according to the Mie theory,[11] produces a value close to 13 (in double pass). Here the main limitation is due to the restricted sensitivity of our camera.

We performed another, more realistic, experiment with the test target placed inside a cell filled with water and 200-nm latex spheres, 1.7 mm behind the front window. We used another CCD camera with a variable exposure time (12-bit Sensys camera). The
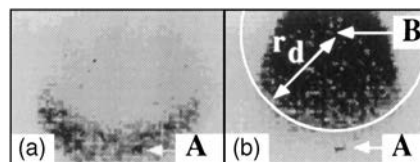

Fig. 2. Amplified spatial frequency spectra in the Fourier plane of lens L_3 of the reflecting diffuser for (a) $\theta_p \approx 42.3°$ and for (b) $\theta_p \approx 41.5°$. Point A corresponds to the pump beam, whereas point B corresponds to the idler wave vector propagating at 2° with respect to the pump wave vector.
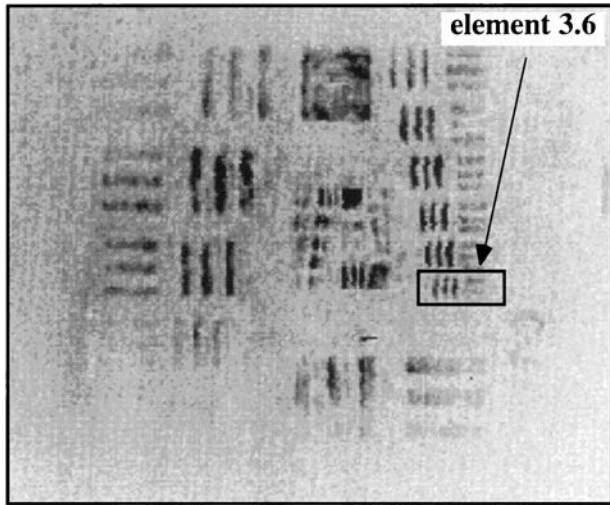
Fig. 3.   Time-gated image of the U.S. Air Force test chart hidden behind a liquid scattering medium of ≈13-mfp scattering depth.
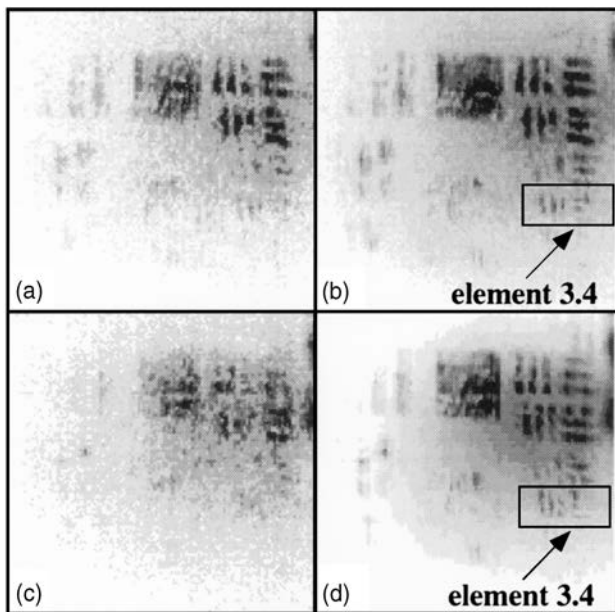

Fig. 4.   Images of the U.S. Air Force test chart hidden 1.7 mm inside the cell through ≈12-mfp scattering depth with (a) 16-ms and (b) 56-ms integration times and through ≈15-mfp scattering depth with (c) 16-ms and (d) 1-s integration times.

limitation of the method then became the speckle noise that is due to the multiply scatted light that leaves the medium during the time gate. Figures 4(a) and 4(b) were obtained for two exposure times from the camera for a scattering medium equivalent to ~12-mfp scattering depth in double pass ($N \approx 3.02 \times 10^{12}$ cm^{-3}). When the target was placed in water the transverse resolution decreased by a factor of 1.33 from that in the previous experiment. Whereas the 90-μm smallest details [element 3.4 in Fig. 4(b)] of the image are resolved for an integration time of 56 ms (averaging of 56 pulses), they become slightly blurred by the speckle for the 16-ms exposure time of our CCD camera (average of 16 pulses). We could observe images with a scattering depths up to 15 mfp when the integration time was increased to 1 s [Fig. 4(d)].

In conclusion, we have demonstrated the feasibility of making depth-resolved 2-D images at video rate through a liquid scattering medium with ≈90-μm lateral spatial resolution and ≈24-μm longitudinal spatial resolution with femtosecond parametric amplification. Further research is now in progress to adapt the method presented here to imaging in solid scattering media such as biological tissues.

C. Doulé's e-mail address is claude.doule@iota.u-psud.fr.

References

1. G. J. Tearney, B. E. Bouma, S. A. Boppart, B. Golubovic, E. A. Swanson, and J. G. Fujimoto, Opt. Lett. **21,** 1408 (1996).
2. A. M. Rollins, M. D. Kulkarni, S. Yazdanfar, R. Ungarunyawee, and J. A. Izatt, Opt. Express **3,** 219 (1998).
3. R. Jones, N. P. Barry, S. C. W. Hyde, P. M. W. French, K. W. Kwolek, D. D. Nolte, and M. R. Melloch, Opt. Lett. **23,** 103 (1998).
4. E. Beaurepaire, A. C. Boccara, M. Lebec, L. Blanchot, and H. Saint-Jalmes, Opt. Lett. **23,** 244 (1998).
5. G. W. Faris and M. Banks, Opt. Lett. **19,** 1813 (1994).
6. K. M. Yoo, Q. Xing, and R. R. Alfano, Opt. Lett. **16,** 1019 (1991).
7. J. Watson, P. Georges, T. Lépine, B. Alonzi, and A. Brun, Opt. Lett. **20,** 231 (1995).
8. F. Devaux, E. Lantz, A. Lacourt, D. Gindre, H. Maillotte, P. A. Doreau, and T. Laurent, Nonlinear Opt. **11,** 25 (1995).
9. C. Yan and J.-C. Diels, Appl. Opt. **31,** 6869 (1992).
10. E. Lantz, L. Han, A. Lacourt, and J. Zyss, Opt. Commun. **97,** 245 (1993).
11. H. C. van de Hulst, *Light Scattering by Small Particles* (Dover, New York, 1982).